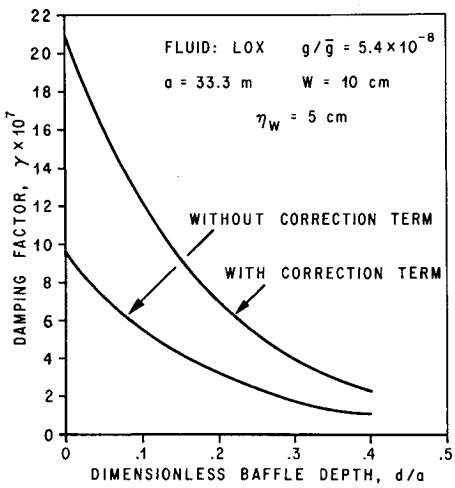

Fig. 2 Effect of Reynolds number correction term.

tank. The result was an expression for the damping provided by one flat ring baffle under high-gravity conditions. One of the most striking differences between high- and low-gravity sloshing is the period of oscillation. In a large tank, like the S-IVB stage of the Saturn V, periods of several hundred seconds[4] have been observed when the vehicle was under vent thrust in Earth orbit. For situations like this, the liquid interface is nearly flat and surface tension effects are small because of the size of the tank. The body forces associated with the applied thrust predominate, and yet are so small that the motion is very slow. A careful examination of these factors reveals that the technique used by Miles is still applicable for predicting the damping with reasonable accuracy provided that the drag coefficient data similar to that of Ref. 3 can be found for much lower Reynolds numbers.

Analysis

The experimental investigation reported in Ref. 5 was conducted to obtain drag coefficient data for Reynolds numbers from 1 to 1000. Analysis of the results yielded a functional relationship among the pertinent parameters: the drag coefficient, Reynolds number and the period parameter as shown in Fig. 1.

This functional relationship may be expressed mathematically in explicit form as follows:

$$C_D = 15P_d^{-1/2} \exp(1.88/N_R^{0.547}) \quad (1)$$

where C_D denotes the drag coefficient, $P_d = U_m\tau/W$ the period parameter, and $N_R = U_mW\rho/\mu$, the Reynolds number. Equation (1) was derived from a curve fitted by eye to the experimental data for Reynolds number ranging from 2 to 1.4×10^4.

According to Miles' analysis,[2] an expression for damping, γ, in terms of drag coefficient C_D, velocity potential ϕ, baffle geometrical parameter α, and wave amplitude parameter, η_w/a may be written

$$\gamma = C_D\phi(\eta_w/a)\alpha \quad (2)$$

where $\alpha = (2aW - W^2)/a^2$. In the expression for damping, γ is equivalent to the logarithmic decrement divided by 2π. For the particular case of a right circular cylinder filled with liquid and having a single ring baffle well beneath the liquid free surface, Eq. (2) was shown to become

$$\gamma = 0.5 \exp(-5.52d/a)\alpha C_D(\eta_w/a) \quad (3)$$

where d/a denotes the baffle depth parameter.

Assuming that Miles' argument for adapting the flat plate results for ring damping is also valid for low Reynolds numbers, Eq. (1) may be substituted into Eq. (3):

$$\gamma = 7.5\alpha(\eta_w/a)P_d^{-1/2} \exp(N_R^{1.88/0.547} - 5.52d/a) \quad (4)$$

By including an additional term for Reynolds number in the exponent of Eq. (4) the range of application of the damping coefficient γ has been extended to low Reynolds numbers. In Fig. 2, damping factor is presented as a function of fluid depth over the baffle for both a case including the correction term and one without it. As can be seen by comparison of the two curves for large tanks at low-g levels, the relative effect of Reynolds number can be significant. The equation should not be applied to cases in which the interface is highly curved since the potential solution used in the analysis is not applicable, a good indication of the degree of surface curvature is provided by Bond number; high Bond number—interface flat, low Bond number—highly curved. However, for Bond numbers greater than 50 and Reynolds numbers smaller than 100, this expression should provide accurate results.

References

[1] Dodge, F. T. and Garza, L. R., "Simulated Low-Gravity Sloshing in Cylindrical Tanks Including Effects of Damping and Small Liquid Depth," TR 5, Dec. 1967, Southwest Research Institute, San Antonio, Texas.

[2] Miles, J. W., "Ring Damping of Free Surface Oscillations in a Circular Tank," *Transactions of the ASME: Journal of Applied Mechanics*, Vol. XXV, June 1958, pp. 274–276.

[3] Keulegan, G. H. and Carpenter, L. H., "Forces on Cylinders and Plates in an Oscillating Fluid," *Journal of Reseacrh of the National Bureau of Standards*, Vol. LX, 1958, pp. 423–440.

[4] Buchanan, H. J. and Bugg, F. M., "Orbital Investigation of Propellant Dynamics in a Large Rocket Booster," TN D-3968, May 1967, NASA.

[5] Buchanan, H., "Drag on Flat Plates Oscillating in Incompressible Fluid at Low Reynolds Numbers," M.S. thesis, 1968, Univ. of Alabama in Huntsville, Ala.

Thermionic Reactor Ion Propulsion Spacecraft for Unmanned Outer Planet Exploration*

J. F. Mondt* and J. P. Davis†
Jet Propulsion Laboratory, Pasadena, Calif.

THE nuclear thermionic reactor power system is one of the leading nuclear power system candidates for electric propulsion applications for unmanned missions to Jupiter, Saturn, Uranus, and Neptune. Nuclear thermionic power systems (like solar power systems) consist of many static power conversion modules arranged to tolerate module failures. The

Presented as Paper 70-1122 at the AIAA 8th Electric Propulsion Conference, Stanford, Calif., August 31–September 2, 1970; submitted September 30, 1970; revision received November 30, 1970. This work presents the result of one phase of research carried out in the Propulsion Research and Advanced Concepts Section of the Jet Propulsion Laboratory, California Institute of Technology, under Contract NAS7-100, sponsored by NASA.

* Leader, Thermionic Reactor Systems Project.

† Presently employed as Special Project Staff, Thermo Electron Corporation, Boston, Mass.

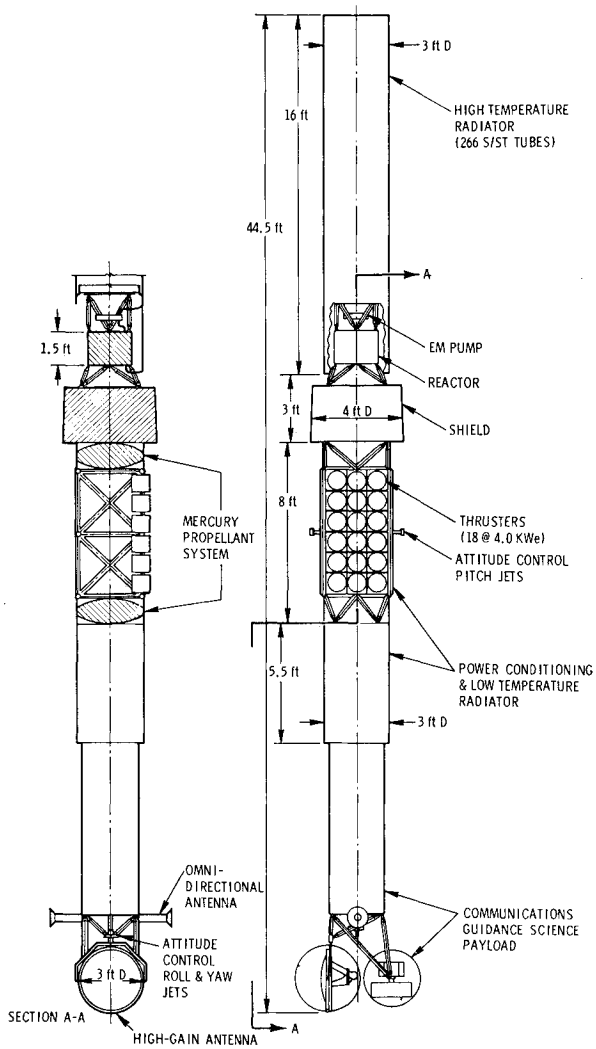

Fig. 1 Side thrust spacecraft arrangement.

external-fuel thermionic reactor coolant system is also arranged to tolerate loss of coolant from punctured radiator tubes, weld leaks, etc. The thrusters and power conditioners also are modularized and arranged to tolerate module failures. This approach and a conservative initial operations mode greatly increase the probability of mission success. At the 70-kw$_e$ power level, low specific weights also are achievable.

A spacecraft arrangement with a large length to diameter ratio ($L/D \cong 20$) reduces shield weight, bus bar weight, and coolant pipe weight. A 70-kw$_e$ axial thrust spacecraft arrangement with an over-all length of 49.7 ft was described in Ref. 1. The thrusters were located in an annular ring around the spacecraft. The antenna was at one end of the spacecraft and the science payload was at the other end to allow the science payload a 3π-steradian field of view. The disadvantages of such an axial thrust arrangement are: 1) the science payload must be covered during thrust phases to protect the instruments from the mercury exhaust propellant, 2) the high-gain antenna must be thermally insulated from the high-temperature radiator, and 3) a 60-ft electrical cable is required from the science payload to the antenna. This Note describes a side-thrust spacecraft arrangement (Fig. 1) which takes advantage of the lightweight, large L/D spacecraft, but eliminates the foregoing disadvantages.

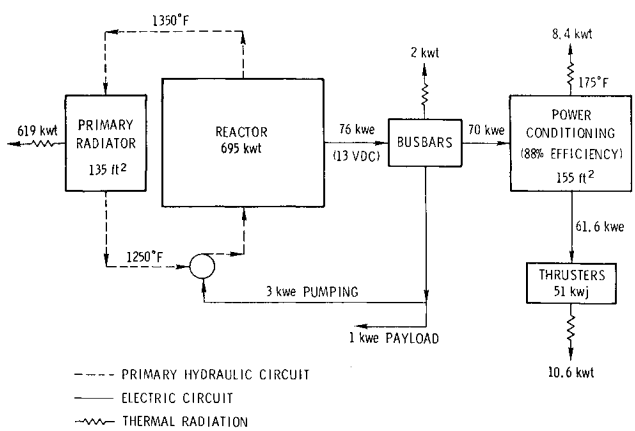

Fig. 2 Power balance and distribution for the 70 kw$_e$ propulsion system.

Table 1 70-kw$_e$ spacecraft weight breakdown, lb

Propulsion system			5,000
Thermionic reactor	1,300		
Heat rejection	1,000		
Nuclear shield	800		
Launch structure	500		
Total power subsystem		3,600	
Power conditioner	650		
Power cables	150		
Thruster array	250		
Launch structure	350		
Total thrust subsystem		1,400	
Low-thrust propellant			3,630
Low-thrust propellant inerts			130
Net spacecraft			2,065
Total spacecraft			10,825
Shroud payload penalty			1,075
Total to Earth escape			11,900

A 3-ft-by-3-ft-square by 8-ft-long thruster array section is located in the middle of the spacecraft. The propellant distribution system and a portion of the power conditioner (P/C) are also in the thruster array section. A 3-ft-diam by 5.5-ft-long P/C section is directly behind the thruster array section. The net spacecraft, including communications, guidance, controls, and science payload, is all in one section at the end of the spacecraft opposite the high temperature power system. The net spacecraft is shadowed from nuclear radiation by a shield. The propellant located behind the shield, also serves as the gamma shielding.

A preliminary analysis of the spacecraft structure was based on a 5-g lateral load and a 10-g axial load. Bending moment and shear diagrams were used to determine structural member size, skin thickness and basic load paths. Stainless steel is used for the shield, reactor, and high-temperature radiator structure because of the possible 1400°F maximum operating temperature. The P/C structural material is aluminum. The propellant tanks are made of titanium, because aluminum is not compatible with Hg. The launch structure weighs 850 lb. As a result of the structural analysis, a) the high-temperature radiator tube supports and the science support structure have been strengthened, b) the thruster support are made stiff in torsion, c) longerons and bottom stiffeners have been added to the reactor and shield, d) propellant tanks are de-

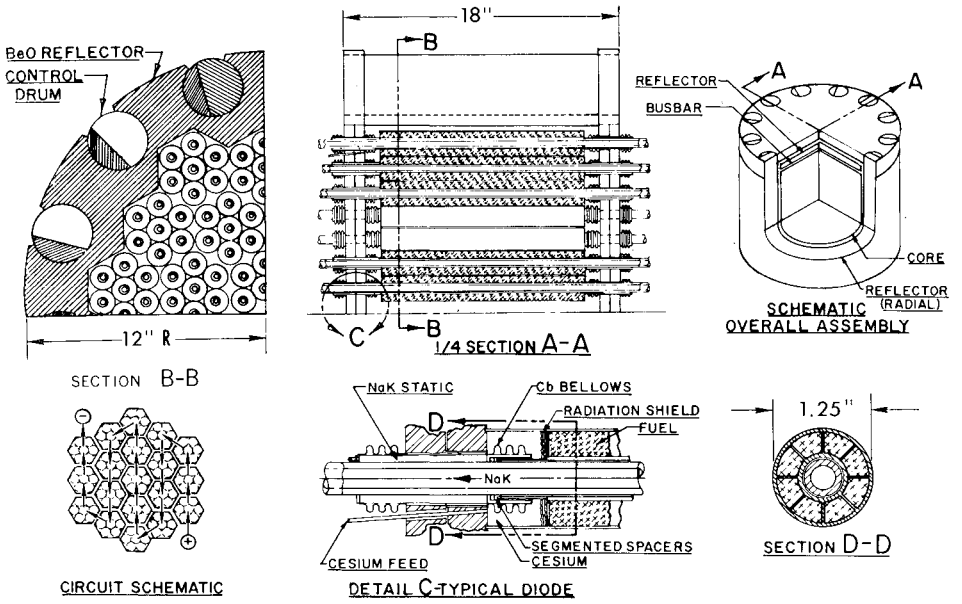

Fig. 3 70 kw_e external-fuel thermionic reactor.

signed with curved ends, e) the shield base includes spacecraft launch attachment bulkheads; and f) welded aluminum tubes are used to support the science payload equipment. The spacecraft's weight breakdown is given in Table 1.

Electric Propulsion System

The power subsystem delivers 70 kw_e to the thrust subsystem, which converts the 70 kw_e to 51 kw_j of thrust. The total propulsion system power balance, from the reactor thermal power (695 kw_t) to the thruster jet power (51 kw_j) is shown in Fig. 2. The propulsion system is designed with a 20% allowance for component failures and/or component performance degradation. Therefore, the power subsystem and thruster subsystem are initially operated at 80% of their capability, which enhances reliability.

The power subsystem consists of a thermionic reactor, a high-temperature primary radiator, a nuclear shield, and an electromagnetic (EM) pump. The 24-in.-diam, 18-in.-long thermionic reactor (Fig. 3) consists of 133 externally fueled, 10-in.-long thermionic converters, each cooled by 0.1 lb/sec of NaK-78 coolant flowing in a 0.30-in.-diam hole through the converter collector. The converter waste heat is radiated to space from 266 stainless steel tubes (0.42-in.-diam $\times$ 0.035-wall) arranged into a 3-ft-diam cylindrical radiator. The NaK is circulated by a multiducted EM pump with 19 electrically isolated pumping sections; each section contains seven hydraulically independent ducts. The external-fuel thermionic reactor can continue to supply 70 kw_e with loss of coolant from 19 primary coolant loops. This greatly increases the power subsystem reliability and mission success probability.

The thrust subsystem consists of eighteen 10-in.-diam, 4-kw_e mercury bombardment thrusters, each having its own P/C. Fifteen thrusters (60 kw_e) will be operating at one time with initially three spares. The thruster propellant utilization and power efficiencies were assumed to be 90% and 92%, respectively. Each thruster weighs 10 lb and operates at a specific impulse of 5000 sec. Mercury was chosen as the propellant because of the well developed technology of mercury thrust systems. The P/C components, using silicon transistors, are mounted on aluminum panels which reject heat directly to space. The transistor hot-spot temperature is maintained below 200°F. The P/C design[2] is based on prototype equipment being used in the Solar Electric Propulsion System Technology (SEPST) Program.

Launch Vehicle

The Titan III-D/Centaur (the basic Titan vehicle with two 5-segment solid-fuel strap-on boosters and a Centaur last stage) can boost 12,000 lb to Earth escape. The Centaur structure can withstand the axial launch loads but cannot withstand the bending moment launch loads caused by the 50-ft-long, 70-kw_e spacecraft. Therefore, the Centaur will be covered by a shroud that will carry the bending moment launch loads into the Titan structure.

The proposed spacecraft shroud is divided into a 25-ft-long, 950-lb section tapered from 11-ft to 5-ft diameter, and a 25-ft-long, 532-lb, 5-ft-diam cylindrical section. The tapered section is assumed as launch structure (between the spacecraft and the Centaur). The Centaur shroud (1220 lb) and upper one-half of the spacecraft shroud (532 lb) is assumed to be ejected after Titan shutdown and prior to Centaur startup. The ejected shroud weight penalty for Earth escape payload is $\frac{1}{14}$ of the actual shroud weight, or 125 lb. The tapered shroud section (which must be launched to Earth escape) weight penalty is 950 lb. The total shroud payload penalty is then 1075 lb.

Conclusions

The external-fuel thermionic reactor concept provides the potential for developing a useful 70-lb/kw_e, 70-kw_e electric propulsion system. The side-thrust propulsion system isolates the science payload from the high temperature, the nuclear radiation and the mercury exhaust environments. A spacecraft arrangement using side-thrust propulsion allows a 4π steradian field of view during the entire mission. The Titan III-D/Centaur launch vehicle, being developed for other unmanned missions, has the capability to launch the 70-kw_e spacecraft to Earth escape.

References

[1] Mondt, J. F., "70 kw_e Thermionic Reactor Electric Propulsion Spacecraft," *JPL Space Programs Summary 37-62 Supporting Research and Advanced Development*, Vol. III, Jet Propulsion Lab., Pasadena, Calif., April 30, 1970.

[2] Pawlik, E. V., Costogue, E. N., and Schaefer, W. C., "Operation of a Lightweight Power Conditioner with a Hollow Cathode Ion Thruster," AIAA Paper 70-648, San Diego, Calif., 1970.